GLIA 35:63–71 (2001)

Rumpshaker-Like Proteolipid Protein (PLP) Ratio in a Mouse Model With Unperturbed Structural and Functional Integrity of the Myelin Sheath and Axons in the Central Nervous System

THOMAS USCHKUREIT,[1] OLAF SPÖRKEL,[1] HEINRICH BÜSSOW,[2] AND WILHELM STOFFEL[1]*

[1]*Laboratory for Molecular Neuroscience, University of Cologne, Cologne, Germany*
[2]*Institute of Anatomy, University of Bonn, Bonn, Germany*

KEY WORDS PLP/DM_{20}; gene targeting; *neo*-gene; splicing; mRNA stability; *rumpshaker* phenotype

ABSTRACT The gene *plp* on the X chromosome encodes the isoforms proteolipid protein (PLP) and DM_{20}, two dominant integral membrane proteins of central nervous system (CNS) myelin. DM_{20} results from the activation of the cryptic splice site in exon III of the *PLP* gene. We inserted a *sense*-orientated loxP flanked *neomycin*-gene into intron III of the *plp* sequence, using homologous recombination in embryonic stem cells and generated the homozygous *neoS* mouse line. Unlike the previously described complete PLP/DM_{20} ablation ($plp^{-/-}$), which has been obtained by introducing a *neo*-gene in *antisense*-orientation in the same position of intron III, the *plp* expression surprisingly revealed reduced mRNA levels. The PLP isoform was reduced to 50%, but DM_{20} expression was unaffected. This protein pattern resembles the expression profile of the PLP isoforms in the natural occurring *rumpshaker* mutant. Electron microscopic examination revealed a normal compaction of CNS-myelin and maintenance of axon integrity. PLP expression levels of the *wt* control were recovered by *Cre* excision of the *neo*-selection gene after intercrossing *neoS* mice and oligodendrocyte-specific *Cre*-mice. These data strongly hint at different functions of intron III in PLP/DM_{20}-specific splicing and mRNA stability. Furthermore evidence is provided for functionally affected translation products of the *PLP* gene in the *rumpshaker* mutant, whereas no PLP-isoform occur in $plp^{-/-}$ mice generated by introducing a selectable marker into intron III in *antisense* orientation. *GLIA 35:63–71, 2001.*

INTRODUCTION

Oligodendrocytes spirally enwrap CNS axons and form up to 50 segments between the nodes of Ranvier with the developmentally important insulating properties suited for saltatory conduction. A specific composition of proteins and complex lipids maintains the highly ordered architecture of this multilayered membrane system. Proteolipid protein (PLP, 30 kDa) and its alternative spliced isoform DM_{20} (26 kDa) constitute about 50% of the protein in CNS myelin (Folch and Lees, 1951; Stoffel et al., 1984). The two membrane proteins are integrated into CNS myelin lipid bilayer with a four-helix transmembrane topology (Weimbs and Stoffel, 1992). These membrane proteins play a

Grant sponsor: BMBF/Center of Molecular Medicine (ZMMK); Deutsche Forschungsgemeinschaft; Grant number: SFB 243.

Thomas Uschkureit is currently at the Institut für Neuropathobiologie, ZMNH, Universität Hamburg, Martinistrasse 85, D-20246 Hamburg, Germany.

*Correspondence to: W. Stoffel, Laboratory for Molecular Neuroscience, Institute of Biochemistry, Faculty of Medicine, University of Cologne, Joseph-Stelzmann-Str. 52, D-50931 Cologne, Germany. E-mail: wilhelm.stoffel@uni-koeln.de

Received 28 February 2001; Accepted 11 May 2001

crucial role for adhesion of external membrane surfaces of oligodendrocyte processes ultrastructurally appearing as the electron-dense intraperiod dense line (IDL) (Boison and Stoffel, 1994). The main dense line (MDL) results from adhesive properties of the cytosolic membrane surfaces with myelin basic proteins (MBP) as key players (Kamholz et al., 1986; Privat et al., 1979).

The human gene *plp* is localized on chromosome Xq22.3 and contains seven exons distributed over a range of 17.6 kb (Diehl et al., 1986; Willard and Riordan, 1985). Activation of the alternative splice site leads to the isoprotein DM_{20} (Nave et al., 1987) in which 105 bp of the 3′ end of exon III are deleted. This corresponds to the excision of 35 amino acid residues within the hydrophilic cytosolic loop of the four transmembrane helix (TMH) model.

PLP shows a high degree of evolutionary conservation among different species (Schliess and Stoffel, 1991; Stecca et al., 2000; Yoshida and Colman, 1996). The highly conserved structure of the proteolipids is a reasonable explanation for the critical susceptibility of the polypeptide to mutations in the *PLP* gene. Most of the naturally occurring mutant forms of PLP, like the *jimpy*-mouse (Nave et al., 1986), the *md*-rat (Boison, 1989) or several X-linked human sudanophilic leukodystrophies (Pelizaeus-Merzbacher disease, reviewed in Gow et al., 1996; Yool et al., 2000), are associated with premature death of oligodendrocytes and CNS hypomyelination often incompatible with the viability of the individual. Exceptions of the observed neuropathological phenotype are other natural mutants, e.g., the *rumpshaker* mouse and the *paralytic tremor* rabbit (Fanarraga et al., 1992; Tosic et al., 1993). The *rumpshaker* mutation causes a marked hypomyelination associated with a reduction in PLP protein but no apparent loss of oligodendrocytes (Schneider et al., 1992). *Rumpshaker* mice therefore provide a model for spastic paraplegia (SPG2) and milder forms of PMD (Yool, 2000) although a recent report suggests that *rumpshaker* may share more characteristics with the juvenile-lethal *plp* mutations than has previously been recognized (Billings-Gagliardi et al., 2001).

In a previous study, we generated a PLP-deficient ($plp^{-/-}$) mouse line by the gene targeting approach using a replacement construct with the selection marker (*neo)* inserted in reverse orientation into intron III (Boison and Stoffel, 1994). The complete deficiency of the translation products in this knockout mouse line is associated with aberrant spliced RNA resulting from the integration of the selection marker and followed by a postulated synthesis of antisense RNA and the immediate degradation of double-stranded RNA formed (Boison and Stoffel, 1994; Boison et al., 1995). The deficiency of the proteolipid protein isoforms in the myelin membrane interfered with the stable adherence of the outer adjacent membrane surfaces of CNS myelin to form the compact intraperiod dense lines. Unlike the well-characterized point mutations of the *PLP* gene the PLP-deficient mice show only very mild neuromotor symptoms, they reproduce normally and have a full life span (Boison et al., 1995).

In the present study, we integrated the lox P-embraced *neo*-cassette in sense orientation into intron III of the murine *PLP* gene by homologous recombination. PLP expression in resulting *neoS* mice is reduced by 50% and therefore resembles that described in the natural occurring *rumpshaker* mutant but unlike *rumpshaker* mutants CNS-myelin sheath of the *neoS*-mouse is properly compacted and maintained during the lifetime of mutant mice. The differences in amount of mRNA and protein arise from a splice defect similar to that observed in $plp^{-/-}$ mice. PLP- and DM_{20}-specific transcripts indicate a different stability in the respective specific hn-RNA molecules, with the PLP primary transcript less stable than the DM_{20} hnRNA.

MATERIALS AND METHODS

Targeting Construct

The vector pPLP25sL2neoTK has been constructed by standard cloning techniques (Sambrook et al., 1989). It contains 6.7 kb of the murine genomic PLP sequence including exon II up to exon V. A 1.2-kb *Bam*HI/ *Sal*I neo-fragment inserted in intron III in sense orientation was obtained by PCR, using oligonucleotides with appropriate restriction sites for cloning in the original *Bam*HI site. The thymidine kinase (*tk*) gene (pIC19r-MCI-*tk*) flanked the 5′ end of the insert. The targeting construct was linearized with *Hpa*I engineered in the *Nco*I site of exon V.

Generation of *neoS* Mice

A total of 10^7 R1 cells [(129/j × 129sv-cp) F1 background] (kindly provided by A. Nagy, Mount Sinai Hospital, Samuel Lunenfeld Research Institute, Toronto) were electroporated with 25 μg of the linearized targeting vector using a Bio-Rad gene pulser at 230 V and 500 μF. ES cells were grown on mitomycin C-treated G418-resistant mouse fibroblasts (Robertson, 1987). Resistant clones were picked after 8–10 days, expanded and their DNA analyzed by Southern blot analysis. Positive clones were detected by *Hin*dIII and *Eco*RI RFLP monitored with the external ^{32}P- labeled probe plp57 as well as by PCR analysis using the oligonucleotides neo-s (see RT-PCR analysis) and HRA (downstream *PLP* primer: 5′-TCAGCTGTTTTGCAGATGGACAGAAGGTTGG- 3′).

Three correctly targeted ES cell clones were used for blastocyst injection (CD1) (Bradley et al., 1984). One of three injected clones yielded three germline chimeras. Offspring was intercrossed and littermates genotyped to obtain the homozygous transgenic mouse line (*neoS*).

Generation of *Cre*$^{+}$/*neoS*$^{+/+}$ mice

The *neoS*-mutant mouse line was crossed with a mouse line that expressed the *Cre* transgene under the control of the MBP-promoter in a tetracycline dependent manner (Gossen and Bujard, 1992; Gossen et al., 1995). This Cre-mouse has been generated in our laboratory for conditional *gene targeting* experiments. In this study, we used this *Cre*$^{+}$/*neoS*$^{+/+}$ mouse mutant for maximal Cre-activity to achieve the oligodendrocyte-specific excision of the *neo* marker-gene. The genotype of *Cre*$^{+}$/*neoS*$^{+/+}$ mice was confirmed by Southern blot analyses using a 400-bp *Bam*HI Cre fragment (from pBS185; Sauer, 1993) and a transactivator-fragment (from pUHD15-1; Gossen and Bujard, 1992) as hybridization probes, respectively.

RNA Analysis

Total RNA of 15- to 25-day-old mouse brain was isolated by the guanidinium thiocyanate/phenol method (Chomczynski and Sacchi, 1987); 20 μg of RNA were separated on 1.5% agarose/ formaldehyde-gels and blotted onto nitrocellulose (Gene Screen, DuPont). After baking for 2 h at 80°C, the membrane was prehybridized in 50% formamide, 1M NaCl, 1% SDS, and 100 μg/ ml salmon sperm DNA for 4 h at 42°C and hybridized in the presence of 10% dextrane sulfate and the appropriate ^{32}P-labeled probes. Poly(A)$^{+}$ RNA was isolated by affinity purification on oligo(dT)-cellulose according to the manufacturer's protocol (Boehringer-Mannheim). 2 μg of poly(A)$^{+}$ and 5 μg of poly(A)$^{-}$ RNA was separated and hybridized as described above.

Hybridization Probes

The following fragments were ^{32}P-labeled with the random priming DNA labeling kit (Boehringer-Mannheim) according to the manufactures recommendations and used as hybridization probes: a 1,500-bp genomic PCR fragment (plp57) containing sequences from exon V up to exon VII, a 1,362-bp *Pst*I fragment of human PLP cDNA, a genomic 1,300-bp fragment containing the sequence of intron three, a 700-bp *Nco*I *neo* fragment, and a 550-bp *Hin*dIII and *Xba*I fragment of human liver glyceraldehyde-3-phosphate dehydrogenase cDNA (Arcari et al., 1984). Fragments were purified using the Qiaex gel extraction kit (Qiagen). Hybridization signals were recorded with a PhosphorImager (Molecular Dynamics).

RT-PCR Analysis

For reverse transcription, 1 μg of total mouse brain RNA was transcribed in 1× first-strand buffer (Life Technologies, Gaithersburg, MD), 5 μM p(dN)$_6$ (Boehringer-Mannheim), 1 mM DDT, 20 U RNAsin, 1 mM dNTP, and 100 U reverse transcriptase Superscript (Life Technologies), in a total volume of 10 μl for 2 h at 37°C. The following primers were used for the PCR reaction (5′→3′): ExII: GCTTGTTAGAGTGTTGTGCTAGATGTCTGG, ExIVas: CATACAACAGTCAGGGCATAGGTGATGC, ExVIIas: TTGTAAGTGGCAGCAATCATGAAGGTGAGC, neo-s: TAAAACGCACGGGTGTTGGGTCGTTTGTTC, neo-as: AATCCATCTTGTTCAATGGCCGATCCCAT, GAPDHs: GGCAAGGTCATCCATCACAACTT, GAPDHas: TTTCTTACTCCTTGGAGGCCATGT. (5′→3′). The PCR-reaction was performed in a total volume of 100 μl with 10 pmol of each primer, 1 mM $MgCl_2$, 10 mM dNTP, 1× Taq polymerase buffer and 2,5 U Taq-Polymerase (Life Technologies). PCR-cycling was at 95°C for 60 s, 66°C for 45 s, and 72°C for 45 s for different numbers of cycles.

Protein Analysis

Myelin was isolated from homogenized brains in 0.32 M sucrose (Norton and Poduslo, 1973). Equal amounts of protein were separated on 15% sodium dodecyl sulfate-polyacrylamide gel electrophoresis (SDS-PAGE). Myelin proteins were visualized with Coomassie Brilliant Blue (30 μg /lane) or by silver staining (5 μg /lane). Proteins were transferred to nitrocellulose (BA-S 85, Schleicher and Schüll) by semidry electroblotting and individual proteins visualized by Western blot analysis with SuperSignal Substrate (Pierce, Rockford, IL) using a 1:400 dilution of an anti-PLP antiserum (directed against the whole protein) generated in our laboratory (Towbin et al., 1979).

Semiquantitative Analysis

Stained protein and RNA gels were photographed with a gel documentation system (GDS 7500, Ultra Violet Products Ltd) and quantitated with the ImageQuaNT software (Molecular Dynamics).

Electron Microscopy

Homozygous, heterozygous *neoS*$^{-}$ and *wt* mice, 1 and 10 months of age, were anesthetized with Nembutal and perfused with 6% glutaraldehyde in phosphate-buffered saline (PBS) via the left cardiac ventricle. Cervical segments of the spinal cord and the optic nerve were isolated, postfixed in 1% phosphate-buffered OsO_4 in 0,1 M sucrose, and embedded in Epon 812. Ultrathin cross sections of optic nerve and spinal cord were contrasted with uranyl acetate and lead citrate and examined as described (Bussow, 1978).

RESULTS

Homologous recombination in embryonic stem cells was achieved with a gene targeting construct that car-

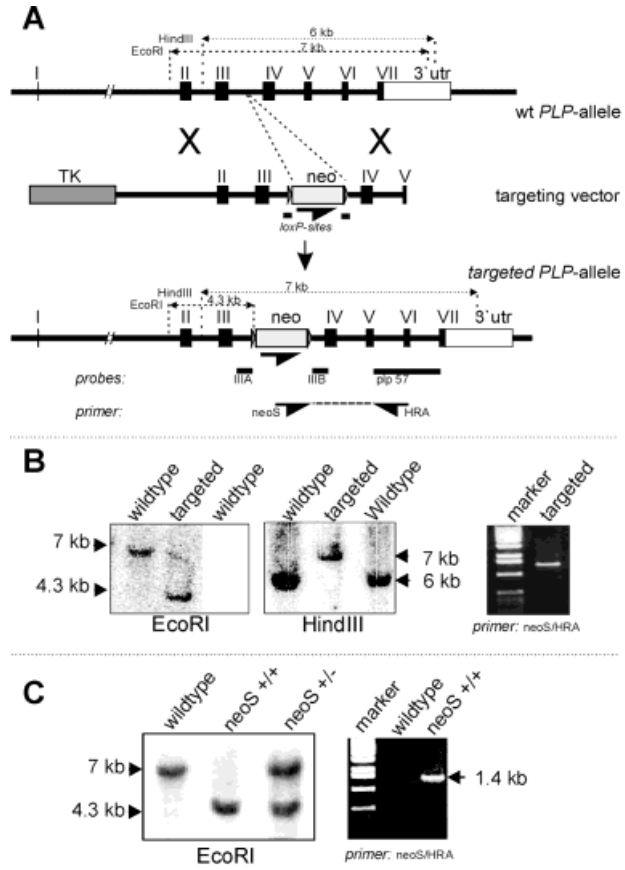

Fig. 1. **A:** Organization of the *plp*-allele of the mouse and the replacement vector containing the HSV-tk gene, and the neo gene inserted into intron III. Targeted mutated *plp*-locus in ES cells. The sites of the primers neoS and HRA as well as the external 3′ probe plp57 and internal neo- and intron III probes. Southern blot hybridization analysis of *Eco*RI and *Hin*dIII restricted genomic DNA of ES-cell clone (**B**), tail DNA of siblings of F1-generation and PCR reaction with primers neo-s and HRA (**C**).

ried the *neomycin* gene in intron III of the mouse *PLP* gene in the orientation of the PLP promoter. This marker gene was flanked by loxP sites (Fig. 1A). ES cell clones with the correctly targeted integration were identified by Southern blot as well as by PCR analysis (Fig. 1B,C). The single integration event was proved by a *neo*-specific hybridization (data not shown). Targeted R1 cells were injected into CD1 blastocysts, and three germline chimeras transmitting the mutation to their offspring were isolated. Finally, the homozygous *neoS*-mouse line was generated by intercrossing the F1 generation (Fig. 1B–D).

As expected from the phenotype of the $plp^{-/-}$ animals homozygous *neoS*-mice showed no behavioral abnormalities. However significant differences in the transcription level of PLP and DM_{20} showed up in Northern blot analysis of total brain RNA of hemizygous, heterozygous, and wt mice. The amount of PLP/DM_{20}-specific transcripts (3.2, 2.4, and 1.6 kb) was reduced by ~50% in homozygous and by 20–30% in heterozygous (data not shown) mutant mice. Signals were standardized to the GAPDH signal (Fig. 2A).

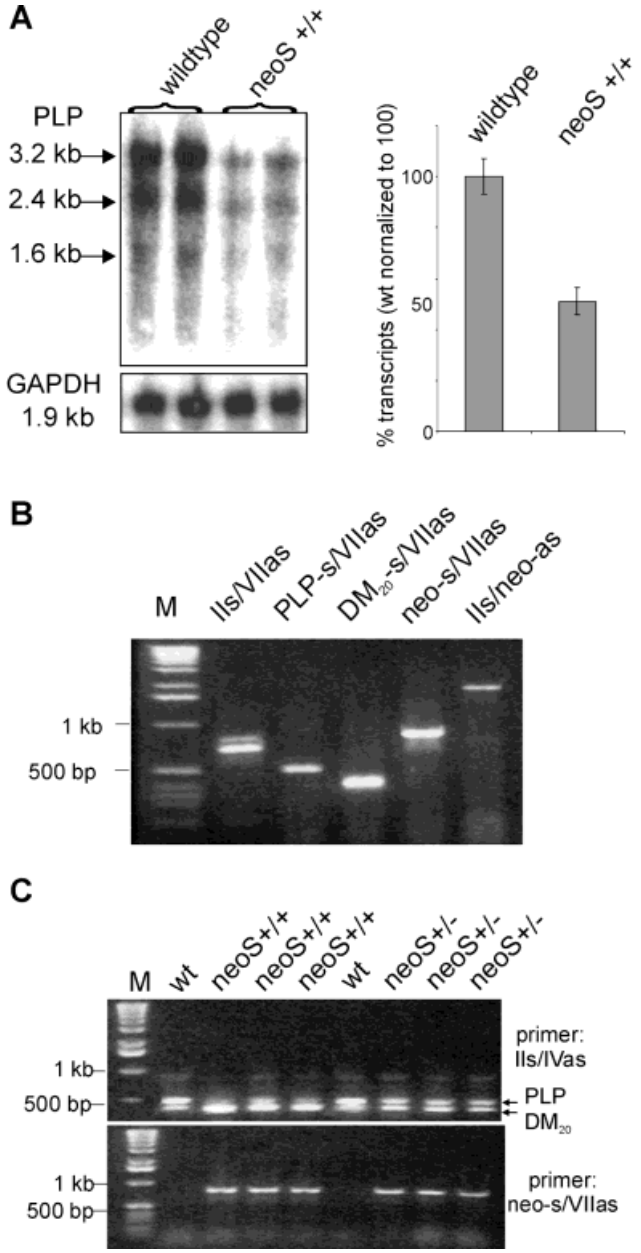

Fig. 2. **A:** PLP-expression in brain of *wt* and $neoS^{+/+}$ mice visualized by Northern blot hybridization using a 1,362-bp *Pst*I fragment of the human PLP cDNA. GAPDH mRNA was used as internal standard. Quantification of ^{32}P-labeled signals of A using a Phosphoimager and the Image Quant software. Intensities are normalized to the intensity of the *wt* hybridization. **B:** RT-PCR using primers indicated to detect neo-, PLP-, and DM_{20} -specific transcripts. **C:** RT-PCR of brain total RNA of *wt*-, hetero- and homozygous *neoS* mice, using PLP- and DM_{20} specific primers for quantification of the ratio PLP/DM_{20} (top), verification of neo-insert using neo-specific primers (bottom).

We investigated *PLP*-gene expression furthermore by RT-PCR analysis (Fig. 2B). Beside the expected cDNA fragments for PLP and DM_{20} we recognized *neo*-specific fragments when primers ExII and neo-as or neo-s and ExVIIa were used for amplification. Sequence analyses identified the occurring PCR products of the corresponding 5′- and 3′-end of the cDNA and

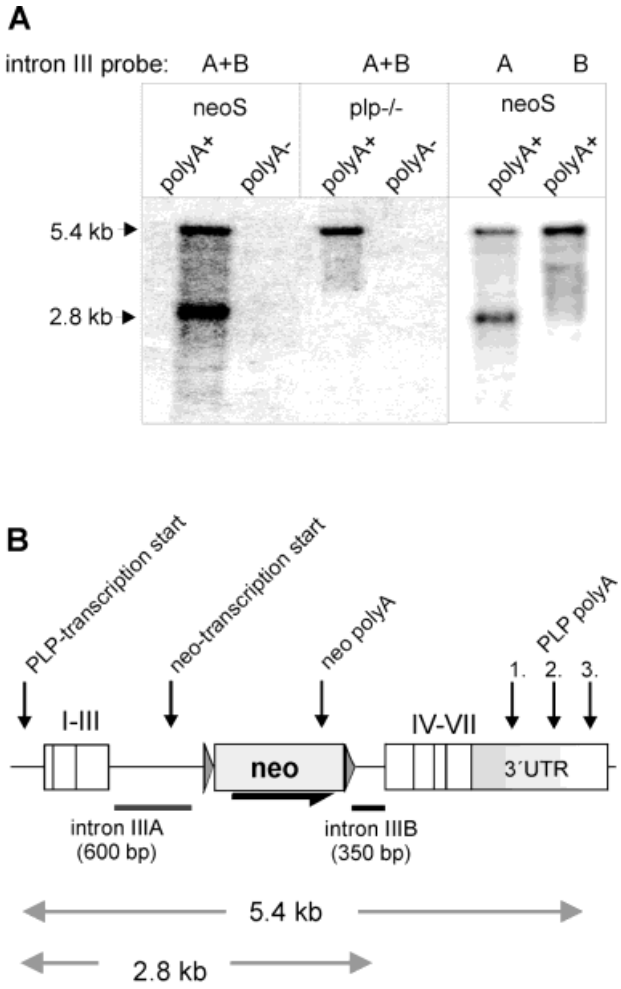

Fig. 3. **A:** Northern blot hybridization analysis. Intron III probes 5′- and 3′ of the *neo* were used to demonstrate the expression of aberrant spliced mRNA. **B:** Schematic representation and interpretation of the aberrant splice products.

intron III-specific sequences, schematically depicted in Figure 3B.

Hybridization of the RNA with probes specific for the *neo*-gene and intron III revealed a 5.4-kb transcript previously described (Boison et al., 1995) and a 2.8-kb transcript corresponding to a transcript starting from the PLP promoter and ending at the polyA signal of the *neo*-gene (Fig. 3A,B). The finding of a hybridized band that migrate with a molecular weight that is consistently lower than predicted could also be explained by initiation of transcription from the *tk* promoter of the *neo*-gene and termination in the 3′UTR of the *plp*-gene. To address this possibilities we generated fragments that are specific for partial sequences of intron III and the origin of the 2.8-kb transcript was determined by an intron III-specific hybridization with these probes indicative for sequences of intron three 5′ and 3′ of the *neo*-gene (Fig. 3A).

Comparative RT-PCR analysis using GAPDH primers as control furthermore indicated that impaired splicing led to a decrease in PLP-specific transcripts and no alterations in DM_{20}-specific transcripts (Fig. 2B). The change in signal intensity of the 600-bp fragment for PLP and the 500-bp fragment for DM_{20} was reproduced with RNA of three different homozygous and *wt*-mice (data not shown).

Myelin of brains of wild-type, $plp^{-/-}$, and mutant *neoS* mice was isolated by sucrose-gradient centrifugation (Norton and Poduslo, 1973). Myelin proteins were size-fractionated by SDS-PAGE and stained with silver (Fig. 4A) as well as Coomassie blue (Fig. 4B). The reduced proteolipid protein in myelin of the *neoS* mouse agreed with the results of the RNA analysis. Otherwise the protein pattern remained unchanged. PLP and DM_{20} bands were normalized to that of proteins with higher (HP) and to low molecular mass (myelin basic proteins) as a control with the appropriate imaging software (ImageQuaNT). These results were further substantiated by Western blot analysis using a purified antiserum raised against the complete PLP, which recognizes both PLP and DM_{20} (Fig. 4C). Comparison of CNS myelin proteins of *wt*, $plp^{-/-}$, and *neoS* mice clearly demonstrate the complete absence of the isoproteins PLP and DM_{20} in $plp^{-/-}$ mice and the decrease in the PLP isoform in the *neoS* -mutant. Taken together, the pattern of the PLP and DM_{20} isoforms of *neoS* mice resembles that described for the natural *rumpshaker* mutant.

While the preceding experiments strongly implicate a *neo*-gene dependent down-regulation of PLP-expression in mutant *neoS* mice, it was unclear whether these findings can be extrapolated to changes in myelin periodicity and myelin maintenance, respectively. We therefore investigated the impact of the change in the PLP/DM_{20} equilibrium in the myelin membrane on myelin periodicity and myelin maintenance, respectively, by electron microscopy. Cross sections of optic nerve and of spinal cord of 1-, 3-, and 12-month-old *neoS* mice show normally compacted CNS-myelin sheaths that were indistinguishable from *wt* control littermates. Also myelin and axonal integrity remained unaltered over a period of 12 months (not illustrated).

For quantitative analysis of total lipids brains of *wt*, $plp^{-/-}$, and *neoS* mice were extracted with chloroform/methanol (2:1), separated by HPTLC. Subsequently the obtained lipids were visualized by charring for all lipids with 50% H_2SO_4. Similar to analyses of myelin of previously analyzed knockout mice no differences in the lipid pattern was detected (data not shown) (Boison et al., 1995; Uschkureit et al., 2000).

In an attempt to reconstitute the PLP synthesis defect in *neoS* oligodendrocytes we eliminated the *neo* marker gene in intron III by crossing an oligodendrocyte-specific Cre-expressing mouse (Cre^{+}) line into *neoS*-mice. This line was generated for conditional *gene targeting* experiments (tetracycline regulated expression). The transactivator (tTA) of the transgene is under the control of the MBP promoter (mbp_{prom}-tTA-cmv^{-1} Cre). In the case of the resulting Cre^{+}/*neoS* mice we used this mutant for tissue-specific Cre-expression despite its applicability for a tetracycline dependent

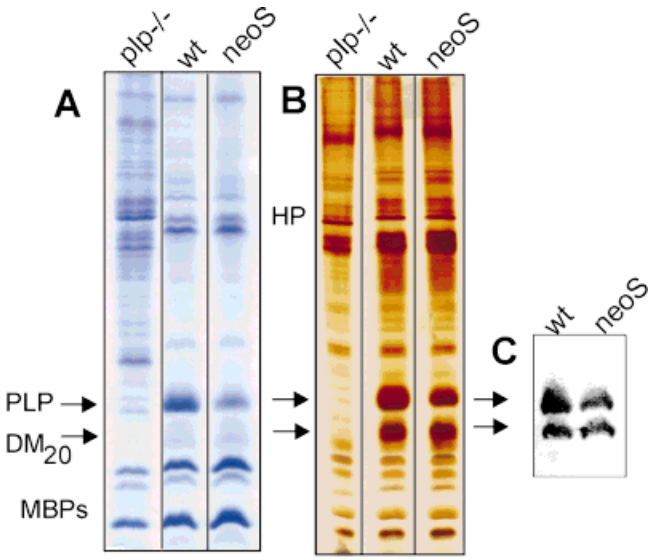

Fig. 4. Coomassie-stained (**A**) and silver-stained (**B**) SDS-PAGE (15%) of purified myelin of *wt*, *neoS* and *plp*$^{-/-}$ mice with anti PLP polyclonal antibodies. **C:** Western blot analysis.

suppression. The genotype of *Cre*$^{+}$*/neoS* mice was confirmed by Southern blot analyses using Cre- and transactivator-specific fragments as hybridization probes (data not shown). To ascertain Cre-activity in *Cre*$^{+}$*/neoS* mice we prepared DNA from brains and a following PCR reaction with primers specific for intron III revealed that Cre-activity in *Cre*$^{+}$*/neoS* mice had released the floxed *neo* gene (data not shown). Oligodendrocyte-specific Cre expression was also documented on the RNA and protein level. PLP/DM$_{20}$-RNA and PLP/DM$_{20}$ proteins were compared in *wt*, *neoS* and *Cre*$^{+}$*/neoS* mice by Northern and Western blot hybridization analyses as well as by a semi-quantitative analysis. Protein and RNA recovery raised to 70–80% in oligodendrocytes of *Cre*$^{+}$*/neoS* mice (Fig. 5A,B,D). Cre-mediated excision of the *neo*-gene was also monitored in polyA^{+} RNA isolated from brains of *Cre*$^{+}$*/neoS* mice using a neomycin-specific probe for Northern blot hybridization. Only traces of the aberrantly spliced 2.8 and 5.4 kb hn-RNA molecules containing parts of intron III were visible (Fig. 5C).

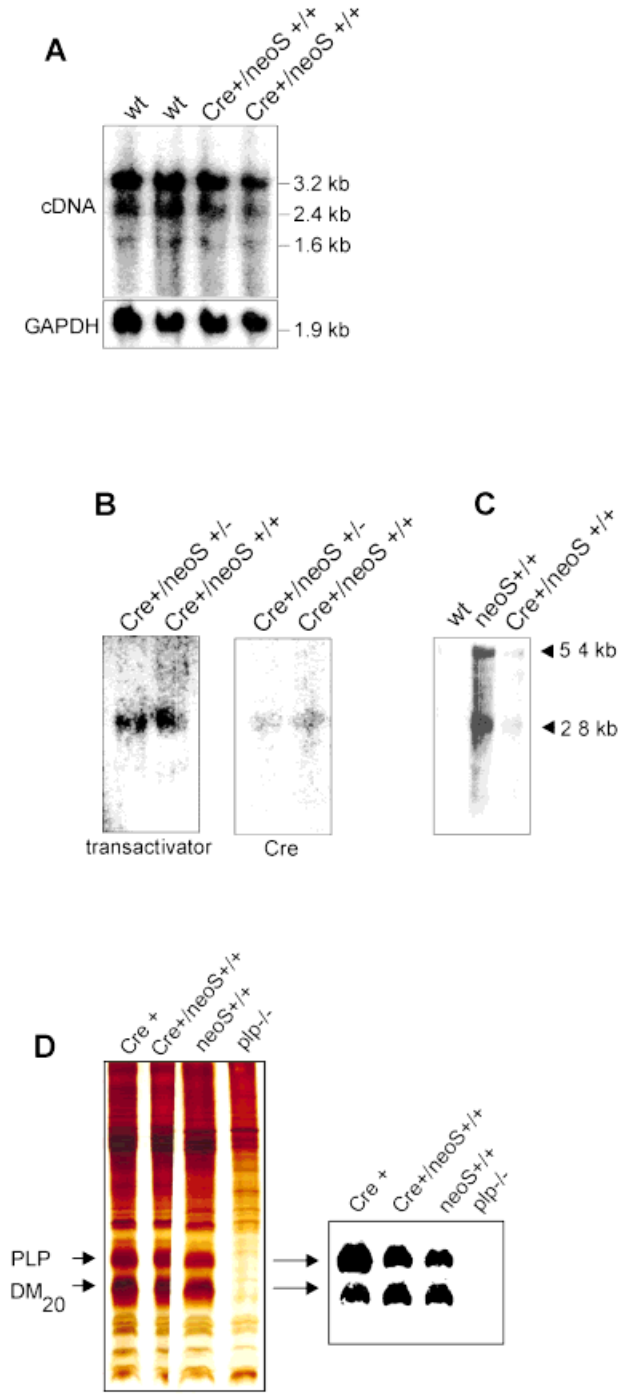

Fig. 5. Comparative analysis of *Cre*$^{+}$*/neoS*$^{+/+}$ mice, *neoS*$^{+/+}$, *plp*$^{-/-}$ and *wt* mice. Northern blot of *plp* transcript (**A**), transactivator and Cre (**B**) and aberrant splice products (**C**). **D:** SDS-PAGE and Western blot of myelin proteins of the four genotypes.

DISCUSSION

Analysis of *PLP* gene expression by homologous recombination of PLP/DM$_{20}$ targeting constructs in embryonic stem cells has proven to be a challenging task to unravel the different functions of the gene products. In previous studies we observed the complete deletion of PLP expression in a mouse mutant the *PLP* gene of which carried the *neo* selection marker in antisense orientation in intron III. To study the effects of the orientation of the *neo* gene selection-marker on *PLP* gene expression, we integrated this additional gene element into intron III of murine *PLP* gene. Surprisingly, the sense-orientated marker-cassette lead to a PLP/DM$_{20}$ isoprotein ratio comparable to that described for the natural occurring *rumpshaker* mouse. This mutant features a 50% mRNA reduction at p20. In the protein analysis PLP is markedly reduced whereas the intensity of the DM$_{20}$ band almost equals that of wt (Mitchell et al., 1992; Schneider et al., 1992). An in-

crease in a presumably proteolipid protein related 10 kDa protein and reduced myelin-specific cerebrosides and sulfatides is observed in the *rumpshaker* mutant mouse (Fanarraga et al., 1992; Karthigasan et al., 1996). X-ray diffraction measurements on unfixed optic nerves furthermore showed that the periodicity in *rumpshaker* CNS myelin is larger than normal (Karthigasan et al., 1996). These biochemical alterations in the *rumpshaker* mutant have been correlated with a wider periodicity and less stable packing of the multilayer myelin sheath. *Rumpshaker* myelin sheaths show variable compaction with occasional myelin vacuolation and intraperiod and major dense lines with indistinguishable electron density (Lunn et al., 1995). These morphological features of the *rumpshaker* mutant resemble those of the $plp^{-/-}$ mouse models (Boison and Stoffel, 1994; Klugmann et al., 1997; Uschkureit et al., 2000) and convincible demonstrated that PLP plays a crucial role in the stability and maintenance of the stable and compact adherence of the outer surfaces of the wrapping oligodendrocyte processes in the IDL.

Unlike the case in *rumpshaker* or knockout mice, the change in the proteolipid protein isoforms in *neoS* mice did not lead to structural and functional alterations of the myelin sheath. Electron microscopic analyses revealed no differences of *neoS* and *wt* myelin, suggesting that neither the reduced concentration nor the altered ratio of the PLP/DM_{20} isoforms interfere with the structure and maintenance of the axonal insulator for at least 12 months.

It has also been suggested that similarities in axon pathology resulting from both decreased (knock out) and increased (transgenics) *PLP*-gene dosages lead to the observed alterations of neuronal integrity (Anderson et al., 1998; Griffiths et al., 1998; Yool et al., 2000). The results derived from the *neoS* mouse model suggest a more sophisticated interpretation: a reduction of PLP down to 50% is compatible with a normal function provided that DM_{20} amounts are unchanged. Our results seem to contradict conclusions drawn from a recently described mouse line that only expresses DM_{20} under the control of the endogenous PLP-promoter (Stecca et al., 2000). These investigators suggest that DM_{20} cannot functionally replace PLP in mice generated by homologous recombination. Our data suggest that diminished amounts of PLP but otherwise unchanged DM_{20} present in CNS myelin do not influence structural or functional properties of this membrane necessary to maintain compacted myelin sheaths.

Despite CNS axons of the *rumpshaker* mutant are hypomyelinated this mutant uncovers a milder phenotype compared to other PLP mutants like the *jimpy*-mouse and the *md*-rat. Surprisingly, when introduced into the C57/Bl6 background the *rumpshaker* mutation produces a severe phenotype (Yool et al., 2000). Another important characteristic of nearly all natural occurring PLP-mutations go along with altered myelin protein and myelin lipid concentrations. In contrast to *neoS* mice, myelin proteins isolated from e.g. *rumpshaker* mutants are in general reduced in amount which suggests that protein targeting is affected in these mutants (Gow et al., 1994, 1998; Mitchell et al., 1992). Furthermore, lipid analysis of *neoS* mice indicates that an impaired protein and lipid translocation is responsible for the observed alterations in *rumpshaker* mice rather than the reduced disproportionate amounts of PLP and DM_{20}. In *rumpshaker* and, e.g., *jimpy* mice, a marked reduction of myelin specific cerebrosides and sulfatides is a common characteristic and probably hint at a delayed maturation of oligodendrocytes (Karthigasan et al., 1996; Yahara et al., 1981).

It should be emphasized that we observed neither myelin abnormalities nor axon degeneration in the *neoS* mutant generated by the targeted alteration of the *PLP* gene, whereas in natural variants mutations in the coding region reduce the synthesis of proteolipid proteins. Mutated PLP and DM_{20} with an abnormal conformation accumulate due to perturbed cellular membrane trafficking (Anderson et al., 1998). An impaired vesicle transfer might block intracellular membrane sorting en route to the plasma membrane and thereby inhibit myelination. This interpretation is supported by the notion that PLP is associated with myelin specific lipids and the report that the cellular distribution of myelin components is altered in a hypo- and demyelinating rat model (O'Connor et al., 2000; Simons et al., 2000).

Another important aspect is oligodendrocyte cell death in mutant mice and human PMD, which generally correlates with the severity of dysmyelination. Dying oligodendrocytes in, e.g., *jimpy* mutants exhibit the classical features of apoptotic cells (Skoff, 1995; Vermeesch et al., 1990). In this regard, it is not surprising that oligodendrocyte survival is not affected in *rumpshaker* mutants since hypomyelination is not as significant as in *jimpy* mice. On the contrary, an increased number of oligodendrocytes in the *rumpshaker* mutant has been observed (Griffiths et al., 1990). Apparently a correlation of oligodendrocyte maturation, survival and/or death and PLP and/or DM_{20} expression does exist. DM_{20} has been proposed to be a likely candidate for a function in oligodendrocyte development distinct from its role in myelin structure, as it is expressed early in development (Nadon and West, 1998). This assumption appears to be confirmed by the *rumpshaker* mutation. In cell culture experiments, *rumpshaker* DM_{20} was almost as effective as *wt* DM_{20} in assisting translocation of rumpshaker PLP to the cell surface (Gow and Lazzarini, 1996). These in vitro results contrast with in vivo findings that *rumpshaker* PLP is not transported efficiently to the oligodendrocyte membrane, as evidenced by the low levels of PLP on the oligodendrocyte surface (Mitchell et al., 1992; Schneider et al., 1992). However, in knockout as well as in *neoS* or Cre^{+}/*neoS* mice there were no changes detectable in oligodendrocyte number or morphology, although these mice express various amounts of the proteolipid isoproteins PLP and DM_{20} (H. Büssow, unpublished observation). Therefore, neither the complete absence nor the reduction of PLP perturbs oligo-

dendrocyte maturation. It is therefore tempting to speculate, that regulatory functions of DM_{20} (PLP) during the ontogenesis of oligodendrocytes can be compensated by redundant functions of other proteins, if any of these proposed functions can be attributed to PLP or DM_{20}.

Crossing the *rumpshaker* mutation into another genetic background produces a severe phenotype which indicates that hypomyelination and oligodendrocyte death are not uncoupled in *rumpshaker* mice (Schneider et al., 1992). We hypothesize that DM_{20} might be involved in the transport of other molecules in addition to PLP, particularly of complex lipids, and that this transport is defective in *rumpshaker* mice. Defective oligodendrocyte maturation therefore seems to be a secondary effect of the mutation.

Another feature of these studies is the different stability of the mutated DM_{20}- and PLP-specific transcripts in *neoS* mutant mice. Although the location and timing of splicing within the nucleus are unknown, the removal of introns has been shown to occur co-transcriptionally. Alterations that retard splicing cause nuclear retention of pre-mRNA and a reduction in the abundance of processed cytoplasmic mRNA. This mechanism of nonsense mediated mRNA decay enables eukaryotes to detect and degrade transcripts harboring premature signals for the termination of translation. In individual cases a decay of 85–95% of the mRNA pool has been observed (Belgrader et al., 1994; Maquat, 1995; Maquat and Carmichael, 2001). Inefficient splicing correlates with a depletion of mutant mRNA and this process is tissue and gene specific (Aoufouchi et al., 1996). Because PLP expression is tightly regulated in oligodendrocytes, inefficient splicing of the PLP transcripts should have significant consequences on PLP expression, as described for *neoS* mice in this study and $plp^{-/-}$ mice previously (Boison and Stoffel, 1994). Furthermore, the hypothesis that antisense RNA is responsible for the knockout phenotype of the $plp^{-/-}$ mouse is supported by the RNA-analysis of *neoS* mice. In the *jimpy* mutant, in contrast to *neoS* and $plp^{-/-}$ mice, defective splicing does not result in a premature stop codon encoded by intron sequences and thus jimpy-mRNA can probably overcome the nonsense mediated decay barrier, which results in the destructive protein structure of jimpy-PLP protein (Nave, 1986).

Little is known about mRNA packaging and export into the cytoplasm. Export requires the disintegration of the multicomponent spliceosome (Brody and Abelson, 1985; Frendewey and Keller, 1985; Hamm and Mattaj, 1990). In case of the *PLP* gene it is very likely that intron III has important functions for PLP- and/or DM_{20}-specific splicing due to positional effects. Intron III-specific spliceosome assembly and disassembly is very likely affected in *neoS* as well as in $plp^{-/-}$ mice. This notion is further supported by the observation that pre-mRNA containing intron III is up-regulated during myelination in a PLP-specific manner (Vouyiouklis et al., 2000). Together with our findings that PLP-specific transcripts are more susceptible to alterations of the structure of intron III are consistent with RNA-stability assays that demonstrate that steady state levels of PLP mRNA are regulated at a posttranscriptional level in Schwann cells, whereas those of DM_{20} are not (Jiang et al., 2000).

It furthermore has to be emphasized that the described results indicate that postulated truncated PLP-like protein products in the comparable $plp^{-/-}$ mouse line (Boison and Stoffel, 1994) are absent and cannot account for observed differences in the two existing knockout mouse lines (Boison and Stoffel, 1994; Klugmann et al., 1997). In contrast, it is very likely that different fixation procedures lead to a misinterpretation of the respective myelin morphology. The procedure used in this study therefore clearly underlines the structural function of the proteolipid proteins since we were unable to detect differences to wt-myelin in *neoS*-mice but clearly showed the disruption of the compacted myelin sheaths as a consequence of protein depletion by the integration of an antisense *neo*-gene into intron III and the following knockout of PLP gene expression (Boison et al., 1995; Uschkureit et al., 2000).

In summary, the insertion of a sense-orientated *neo* gene into intron III of the *PLP* gene (*neoS* mutant) reduces the proteolipid protein isoform in myelin and generates a pattern similar to that of the natural *rumpshaker* mutant. The *rumpshaker* mutation causes a functional defect in myelination. The splice defect in *neoS* mice leads to a considerable reduction of the PLP isoform, but with no effect on compaction and maintenance of the myelin sheaths. Crossing *neoS* mice into oligodendrocyte-specific Cre-mice generated the neoS/Cre mutant. This mutant indicated the scope of the Cre/loxP system for functional studies on the proteolipid protein isoforms.

REFERENCES

Anderson TJ, Schneider A, Barrie JA, Klugmann M, McCulloch MC, Kirkham D, Kyriakides E, Nave KA, Griffiths IR. 1998. Late-onset neurodegeneration in mice with increased dosage of the proteolipid protein gene. J Comp Neurol 394:506–519.

Aoufouchi S, Yelamos J, Milstein C. 1996. Nonsense mutations inhibit RNA splicing in a cell-free system: recognition of mutant codon is independent of protein synthesis. Cell 85:415–422.

Arcari P, Martinelli R, Salvatore F. 1984. The complete sequence of a full length cDNA for human liver glyceraldehyde-3-phosphate dehydrogenase: evidence for multiple mRNA species. Nucleic Acids Res 12:9179–9189.

Belgrader P, Cheng J, Zhou X, Stephenson LS, Maquat LE. 1994. Mammalian nonsense codons can be cis effectors of nuclear mRNA half- life. Mol Cell Biol 14:8219–8228.

Billings-Gagliardi S, Nunnari JJ, Wolf MK. 2001. Rumpshaker behaves like juvenile-lethal Plp mutations when combined with shiverer in double mutant mice. Dev Neurosci 23:7–16.

Boison, D, Stoffel, W. 1989. Myelin-deficient rat: a point mutation in exon III (A–C, Thr75– Pro) of the myelin proteolipid protein causes dysmyelination and oligodendrocyte death. EMBO J 8:3295–3302.

Boison, D, Stoffel, W. 1994. Disruption of the compacted myelin sheath of axons of the central nervous system in proteolipid protein-deficient mice. Proc Natl Acad Sci USA 91:11709–11713.

Boison D, Bussow H, D'Urso D, Muller HW, Stoffel W. 1995. Adhesive properties of proteolipid protein are responsible for the compaction of CNS myelin sheaths. J Neurosci 15:5502–5513.

Bradley A, Evans M, Kaufman MH, Robertson E. 1984. Formation of germ-line chimaeras from embryo-derived teratocarcinoma cell lines. Nature 309:255–256.

Brody E, Abelson J. 1985. The "spliceosome": yeast pre-messenger RNA associates with a 40S complex in a splicing-dependent reaction. Science 228:963–967.
Bussow H. 1978. Schwann cell myelin ensheathing C.N.S. axons in the nerve fibre layer of the cat retina. J Neurocytol 7:207–214.
Chomczynski P, Sacchi N. 1987. Single-step method of RNA isolation by acid guanidinium thiocyanate- phenol-chloroform extraction. Anal Biochem 162:156–159.
Diehl HJ, Schaich M, Budzinski RM, Stoffel W. 1986. Individual exons encode the integral membrane domains of human myelin proteolipid protein. Proc Natl Acad Sci USA 83:9807–9811.
Fanarraga ML, Griffiths IR, McCulloch MC, Barrie JA, Kennedy PG, Brophy PJ. 1992. Rumpshaker: an X-linked mutation causing hypomyelination: developmental differences in myelination and glial cells between the optic nerve and spinal cord. Glia 5:161–170.
Folch F, Lees MB. 1951. Proteolipids, a new type of tissue lipoproteins; their isolation from brain. J Biol Chem 191:807–817.
Frendewey D, Keller W. 1985. Stepwise assembly of a pre-mRNA splicing complex requires U-snRNPs and specific intron sequences. Cell 42:355–367.
Gossen M, Bujard H. 1992. Tight control of gene expression in mammalian cells by tetracycline- responsive promoters. Proc Natl Acad Sci USA 89:5547–5551.
Gossen M, Freundlieb S, Bender G, Muller G, Hillen W, Bujard H. 1995. Transcriptional activation by tetracyclines in mammalian cells. Science 268:1766–1769.
Gow A, Lazzarini RA. 1996. A cellular mechanism governing the severity of Pelizaeus-Merzbacher disease. Nature Genet 13:422–428.
Gow A, Friedrich VL Jr, Lazzarini RA. 1994. Intracellular transport and sorting of the oligodendrocyte transmembrane proteolipid protein. J Neurosci Res 37:563–573.
Gow A, Southwood CM, Lazzarini RA. 1998. Disrupted proteolipid protein trafficking results in oligodendrocyte apoptosis in an animal model of Pelizaeus-Merzbacher disease. J Cell Biol 140:925–934.
Griffiths IR, Scott I, McCulloch MC, Barrie JA, McPhilemy K, Cattanach BM. 1990. Rumpshaker mouse: a new X-linked mutation affecting myelination: evidence for a defect in PLP expression. J Neurocytol 19:273–283.
Griffiths I, Klugmann M, Anderson T, Yool D, Thomson C, Schwab MH, Schneider A, Zimmermann F, McCulloch M, Nadon N, Nave KA. 1998. Axonal swellings and degeneration in mice lacking the major proteolipid of myelin. Science 280:1610–1613.
Hamm J, Mattaj IW. 1990. Monomethylated cap structures facilitate RNA export from the nucleus. Cell 63:109–118.
Jiang H, Duchala CS, Awatramani R, Shumas S, Carlock L, Kamholz J, Garbern J, Scherer SS, Shy ME, Macklin WB. 2000. Proteolipid protein mRNA stability is regulated by axonal contact in the rodent peripheral nervous system. J Neurobiol 44:7–19.
Kamholz J, de Ferra F, Puckett C, Lazzarini R. 1986. Identification of three forms of human myelin basic protein by cDNA cloning. Proc Natl Acad Sci USA 83:4962–4966.
Karthigasan J, Evans EL, Vouyiouklis DA, Inouye H, Borenshteyn N, Ramamurthy GV, Kirschner DA. 1996. Effects of rumpshaker mutation on CNS myelin composition and structure. J Neurochem 66:338–345.
Klugmann M, Schwab MH, Puhlhofer A, Schneider A, Zimmermann F, Griffiths IR, Nave KA. 1997. Assembly of CNS myelin in the absence of proteolipid protein. Neuron 18:59–70.
Lunn KF, Fanarraga ML, Duncan ID. 1995. Myelin mutants: new models and new observations. Microsc Res Tech 32:183–203.
Maquat LE. 1995. When cells stop making sense: effects of nonsense codons on RNA metabolism in vertebrate cells. RNA 1:453–465.
Maquat LE, Carmichael GG. 2001. Quality control of mRNA function. Cell 104:173–176.
Mitchell LS, Gillespie SC, McAllister F, Fanarraga ML, Kirkham D, Kelly B, Brophy PJ, Griffiths IR, Montague P, Kennedy PG. 1992. Developmental expression of major myelin protein genes in the CNS of X-linked hypomyelinating mutant rumpshaker. J Neurosci Res 33:205–217.
Nadon NL, West M. 1998. Myelin proteolipid protein: function in myelin structure is distinct from its role in oligodendrocyte development. Dev Neurosci 20:533–539.
Nave KA, Lai C, Bloom FE, Milner RJ. 1986. Jimpy mutant mouse: a 74-base deletion in the mRNA for myelin proteolipid protein and evidence for a primary defect in RNA splicing. Proc Natl Acad Sci USA 83:9264–9268.
Nave KA, Lai C, Bloom FE, Milner RJ. 1987. Splice site selection in the proteolipid protein (PLP) gene transcript and primary structure of the DM-20 protein of central nervous system myelin. Proc Natl Acad Sci USA 84:5665–5669.
Norton WT, Poduslo SE. 1973. Myelination in rat brain: method of myelin isolation. J Neurochem 21:749–757.
O'Connor LT, Goetz BD, Couve E, Song J, Duncan ID. 2000. Intracellular distribution of myelin protein gene products is altered in oligodendrocytes of the taiep rat. Mol Cell Neurosci 16:396–407.
Privat A, Jacque C, Bourre JM, Dupouey P, Baumann N. 1979. Absence of the major dense line in myelin of the mutant mouse "shiverer." Neurosci Lett 12:107–112.
Robertson EJ. 1987. Teratocarcinomas and embryonic stem cells; a practical approach. IRL Press, Washington, DC.
Sambrook J, Fritsch EF, Maniatis T. 1989. Molecular cloning: a laboratory manual. Cold Spring Harbor, NY: Cold Spring Harbor Laboratory Press.
Sauer B. 1993. Manipulation of transgenes by site-specific recombination: use of Cre recombinase. Methods Enzymol 225:890–900.
Schliess F, Stoffel W. 1991. Evolution of the myelin integral membrane proteins of the central nervous system. Biol Chem Hoppe-Seyler 372:865–874.
Schneider A, Montague P, Griffiths I, Fanarraga M, Kennedy P, Brophy P, Nave KA. 1992. Uncoupling of hypomyelination and glial cell death by a mutation in the proteolipid protein gene. Nature 358:758–761.
Simons M, Kramer EM, Thiele C, Stoffel W, Trotter J. 2000. Assembly of myelin by association of proteolipid protein with cholesterol- and galactosylceramide-rich membrane domains. J Cell Biol 151:143–154.
Skoff RP. 1995. Programmed cell death in the dysmyelinating mutants. Brain Pathol 5:283–288.
Stecca B, Southwood CM, Gragerov A, Kelley KA, Friedrich VL Jr, Gow A. 2000. The evolution of lipophilin genes from invertebrates to tetrapods: DM-20 cannot replace proteolipid protein in CNS myelin. J Neurosci 20:4002–4010.
Stoffel W, Bosio A. 1997. Myelin glycolipids and their functions. Curr Opin Neurobiol 7:654–661.
Stoffel W, Hillen H, Giersiefen H. 1984. Structure and molecular arrangement of proteolipid protein of central nervous system myelin. Proc Natl Acad Sci USA 81:5012–5016.
Tosic M, Dolivo M, Amiguet P, Domanska-Janik K, Matthieu JM. 1993. Paralytic tremor (pt) rabbit: a sex-linked mutation affecting proteolipid protein-gene expression. Brain Res 625:307–312.
Towbin H, Staehelin T, Gordon J. 1979. Electrophoretic transfer of proteins from polyacrylamide gels to nitrocellulose sheets: procedure and some applications. Proc Natl Acad Sci USA 76:4350–4354.
Uschkureit T, Sporkel O, Stracke J, Bussow H, Stoffel W. 2000. Early onset of axonal degeneration in double ($plp^{-/-}mag^{-/-}$) and hypomyelinosis in triple ($plp^{-/-}mbp^{-/-}mag^{-/-}$) mutant mice. J Neurosci 20:5225–5233.
Vermeesch MK, Knapp PE, Skoff RP, Studzinski DM, Benjamins JA. 1990. Death of individual oligodendrocytes in jimpy brain precedes expression of proteolipid protein. Dev Neurosci 12:303–315.
Vouyiouklis DA, Barrie JA, Griffiths IR, Thomson CE. 2000. A proteolipid protein-specific pre-mRNA (Ppm-1) contains intron 3 and is up-regulated during myelination in the CNS. J Neurochem 74:940–948.
Weimbs T, Stoffel W. 1992. Proteolipid protein (PLP) of CNS myelin: positions of free, disulfide- bonded, and fatty acid thioester-linked cysteine residues and implications for the membrane topology of PLP. Biochemistry 31:12289–12296.
Willard HF, Riordan JR. 1985. Assignment of the gene for myelin proteolipid protein to the X chromosome: implications for X-linked myelin disorders. Science 230:940–942.
Yahara S, Singh I, Kishimoto Y. 1981. Levels and syntheses of cerebrosides and sulfatides in subcellular fractions of jimpy mutants. Neurochem Res 6:885–892.
Yool DA, Edgar JM, Montague P, Malcolm S. 2000. The proteolipid protein gene and myelin disorders in man and animal models. Hum Mol Genet 9:987–992.
Yoshida M, Colman DR. 1996. Parallel evolution and coexpression of the proteolipid proteins and protein zero in vertebrate myelin. Neuron 16:1115–1126.